CT Image Segmentation in Traumatic Brain Injury*

S.M.R. Soroushmehr, A. Bafna, S. Schlosser, K. Ward, H. Derksen and K. Najarian

Abstract— **Traumatic brain injury (TBI) is a major cause of disability and death. Speed and accuracy are vital in diagnosing TBI for which computer-aided imaging analysis may speedup and improve the efficiency of diagnosis and help reduce mortality, long-term complications, and the associated costs. However, developing such a system is challenging due to some factors such as the inherent noise associated with obtaining the images, artifacts and quality of the images. An automated system that can preliminary identify, localize and quantify the imaging features of TBI would be beneficial in guiding real-time clinical diagnosis as well as for quality assurance. In this paper we propose an automated system to segment the hematoma region from CT images. The proposed method first performs denoising and image enhancement and then by developing a Gaussian mixture model, segmentation is carried out. We show the performance of the system by comparing the results with ground truth generated by specialists.**

I. Introduction

Traumatic brain injury (TBI) is defined as a blow or jolt to the head that causes temporary or permanent cerebral dysfunction [1]. The total number of traumatic brain injuries occur in the United States alone approaches 3.5 million [2]. A high rate of neurotrauma has been reported for motor vehicle accidents, participation in contact sports and in civilian and military populations in war zones. TBI can cause intracranial hematoma and local tissue disruption, with potential early consequences of brain swelling (edema), and intracranial pressure (ICP) elevation, which lead to further local tissue damage from hypotension and hypoxaemia. TBI can be classified into two main categories; primary injury that happens at the time of impact and secondary injury that develops following the primary injury [3]. Modern neurosurgical care is intended to minimize secondary insults through early detection and effective prevention [3–5]. Cerebral edema, ischemia, and mass effect from hematoma are in the second group [1]. Hematoma is present in around 36% of the patients suffering from TBI [6]. Hematoma can be classified to epidural, subdural, intracerebral, and subarachnoid hematoma based on its anatomic location [2]. Prevention and proper treatment of these sequelae can reduce the injury morbidity, the risk of death, and the cost of care. CT and magnetic resonance imaging (MRI) are among image modalities commonly used for TBI diagnoses. Although MRI has been proven for its greater sensitivity and specificity compared with CT, it is usually used at later stages of treatment when more detailed information is needed. Moreover, MRI it is not routinely used in mild TBI [7]. On the other hand, CT imaging is faster, less costly and can reveal severe abnormalities such as fracture and hematomas [5]. Also, it plays an important role in allowing rapid TBI assessment in the emergency department. Therefore, it is employed as the gold standard in the emergency care for the diagnosis of intracranial injuries following TBI [8]. For instance, the initial assessment and triage of traumatic intracranial hematomas is performed using non-contrast CT scan following injury [9]. It is also used for epidural and subdural hematoma assessment for the patients suffering from TBI [6]. Visual examination of these images might be time consuming, costly and associated with error specially when a large number of images need to be assessed. Computer-aided imaging analysis may improve the efficiency of diagnosis and help reduce mortality, long-term complications, and the associated costs.

In order to segment the hemorrhage regions, Soltaninejad *et al*. partitioned an image to super-pixels and then applied a level set method [10]. In [11], a method proposed for hemorrhage segmentation by modifying *distance regularized level set evolution* (DRLSE) algorithm [12] that doesn't need the reinitialization step required typically in level set methods. DRLSE is a segmentation method that tries to maintain the regularity of the level set function during the level set evolution instead of developing irregularities. Li *et al.* developed a supervised learning method to recognize subarachnoid space (SAS) [13] using the probability of distance features. In this method at first landmarks consisting of brain boundary, midsagittal plane (MSP), anterior and posterior intersection points of brain boundary with the MSP, and superior point of the brain are extracted and then distances between each pixels of the CT image and different landmarks are calculated and considered as a feature vector. Also, for creating the training dataset, the prior probabilities of distances for pixels within SAS and non-SAS are calculated using with manually delineated SAS from CT images. Another approach towards enhancing the hemorrhage area in the brain and hence improving the segmentation accuracy is by denoising the image proposed in [14] followed by a region growing scheme. In order to detect and quantify the hemorrhage between the brain spaces an adaptive thresholding scheme and case-based reasoning have been developed in [15]. The threshold is calculated based on local contrast with different window sizes and is utilized to generate candidate regions showing hemorrhage. These regions are classified using a case-based reasoning approach.

In this paper we propose an automated segmentation of CT brain images of the patients with TBI for detecting hematoma. In this method we utilize Gaussian mixture model (GMM) with four inputs including a raw CT image and its corresponding

* This material is partially based upon work supported by the National Science Foundation under Grant No. IIS0758410.

S. M. R. Soroushmehr, is with the University of Michigan Center for Integrative Research in Critical Care (MCIRCC) and the Emergency Medicine Department, University of Michigan, Ann Arbor, MI.
(e-mail: ssoroush@med.umich.edu)
A. Bafna is with the Electrical Engineering and Computer Science Department, University of Michigan, Ann Arbor, MI.
(e-mail:abafna@umich.edu)
S. Schlosser is with the NovoDynamics Inc., Ann Arbor, MI, USA.
(e-mail: steve@novodynamics.com)
K. Ward is with the University of Michigan Center for Integrative Research in Critical Care (MCIRCC) and the Emergency Medicine Department, University of Michigan, Ann Arbor, MI. (email: kward@med.umich.edu)
H. Derksen is with the University of Michigan Center for Integrative Research in Critical Care (MCIRCC) and the department of Mathematics, University of Michigan, Ann Arbor, Michigan, Ann Arbor, USA.
(e-mail: hderksen@umich.edu)
K. Najarian is with the department of Computational Medicine and Bioinformatics as well as University of Michigan Center for Integrative Research in Critical Care (MCIRCC) and the Emergency Medicine Department, University of Michigan, Ann Arbor, MI.
(e-mail:kayvan@med.umich.edu)

enhanced and denoised images. The segmentation is followed by a post-processing method in which we use statistical properties of the image to remove the segments non-relevant to hematoma.

The rest of the paper is organized as follows. Details of the proposed method are presented in Section II. We show the performance of the proposed method in Section III and finally we conclude the paper in Section IV.

II. Proposed Segmentation Method

The current detection of hematoma is based on visual descriptors. The underlying assumption is that the area containing a hematoma would have higher average intensity than the rest of the brain. However, this is not a sufficient assumption for hematoma detection as the boundary or other parts of the image, which are not diagnosed as hematoma, might have similar pixel values to hematoma. In order to detect the hematoma, input images need to be processed. In our proposed method we first perform a pre-processing stage and then segmentation is carried out using a GMM. After segmenting the image we perform post-processing to remove false positive such as very small regions and the boundary of the image which have similar intensity values as the hematoma region. The block diagram of the proposed method is given in Figure.1 and the details of the method are described in the following.

A. Pre-processing

The input image used here is derived from the slice selection algorithm (SSA) [16] that selects the slices based on the area of intracranial and amount of interference from organs such as eyes and the nose. In the first step of the SSA, each slice is segmented to bone and none-bone regions and then by analyzing the size and number of connected components and also the intracranial area, slices are selected.

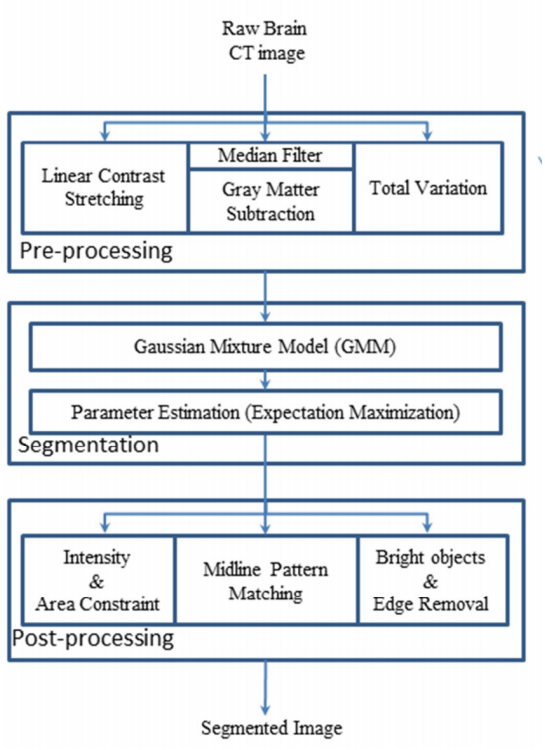

Figure 1. Block Diagram of the proposed method.

The goal of preprocessing is to generate useful features for segmentation. Here, we perform three stages as follow:

1. Linear contrast stretching: This technique enhances the high intensity regions and is applied either to the original image or the output of the GMS stage, forming one of the major inputs to segmentation based on the following equation.

$$f_{enh}(x,y) = H\big(f(x,y)\big) \quad \text{where}$$

$$H(z) = \begin{cases} 0, & z < t_1 \\ g_{max}\ , & z \geq t_2 \\ \dfrac{g_{max}}{t_2 - t_1} \times (z - t_1), & O.W. \end{cases} \qquad (1)$$

In Eq (1), f is the raw input brain CT image or the output of GMS. Also, $[t_1, t_2]$ is the range of pixel values belonging to the object of interest in image f. For example, pixels with the lowest and highest intensity values don't correspond to hematoma regions. Therefore, t_1 can be assigned with a small value higher than the minimum pixel value of the image. Likewise, t_2 is set with a high value smaller than the maximum pixel value of the image. Also, g_{max} is the maximum desired intensity value assigned to the output image. It is assumed that the lowest intensity value in the output image is zero.

2. Gray matter subtraction (GMS): In this stage the gray matter intensity is removed from the image by subtracting the maximum intensity level of the histogram from the image. The input of this stage is the output of the median filter of the raw CT image. The size of the window in the median filter is 3×3.

3. Total Variation (TV): CT images usually contains noise. Therefore, it is essential that we first reduce the amount of noise. The intuitive approach for reducing the noise and preserving important information is the TV denoising model that minimizes the total variation norms which are essentially L_1 norms of derivatives [17]. In this method, denoising is performed by minimizing a least square function with total variation regularization term. The basic model is the minimization problem shown as [17]:

$$\min_u\Big(\int_\Omega |\nabla u| + \lambda ||u - f||_2^2\Big) \qquad (2)$$

where Ω is the image domain, f is the noisy image, λ is the Lagrange multiplier or the regularization parameter and $\int_\Omega |\nabla u|$ is called the total variation of u. It is assumed that $f = u + \eta$ where η is a zero-mean Gaussian random variable showing the noise. A dual formulation of this problem proposed in [18] in which the dual energy of the cost function is less nonlinear than the primal one. This dual model is solved using a primal-dual hybrid gradient descent (PDHGD) method [19]. This descent-type algorithm alternates between the primal and dual formulations and exploits the information from both the primal and dual variables. Therefore, it is able to converge significantly faster than either of them. In this paper we use PDHGD as the denoising technique.

B. Segmentation

Hematoma detection can be broadly regarded as a segmentation problem based on the intensity of the affected regions as it occurs in regions with similar intensity values. For

the segmentation purpose, we apply Expectation Maximization (EM) on a Gaussian Mixture Model (GMM) [18]. Here, we define a GMM by taking 4 components of Gaussian density with parameters mean, $\boldsymbol{\mu_k}$, and covariance, $\sum_k$. Then, the density of each component is calculated using:

$$p_k(\boldsymbol{x}, \boldsymbol{\theta}_k) = \frac{1}{(2\pi)^{d/2}|\sum_k|^{0.5}} e^{-\frac{1}{2}(\boldsymbol{x}-\boldsymbol{\mu_k})^t \sum_k^{-1}(\boldsymbol{x}-\boldsymbol{\mu_k})}, \quad \boldsymbol{\theta}_k = \{\boldsymbol{\mu}_k, \sum_k\} \tag{3}$$

The EM algorithm for Gaussian mixtures is defined as follows [8]. The algorithm starts from some initial estimates of parameter vector $\boldsymbol{\theta}$ and then iteratively updates them until convergence is reached. Each iteration consists of an E-step and M-step as described below.

E-Step: For each data point we compute the membership weights corresponding to each mixture component, w_{ik}. Note that for each data point $\boldsymbol{x_i}$ the membership weights are such that $\sum_k w_{ik} = 1$.

M-Step: Here, the membership weights are used to calculate the new parameter values. If we assume that the sum of membership weights for the k^{th} component is $N_k = \sum_{i=1}^{N} w_{ik}$ then the update mean and covariance matrices are respectively given by Eq (4) and Eq (5) as follow.

$$\boldsymbol{\mu_k}^{new} = \frac{1}{N_k}\sum_{i=1}^{N} w_{ik}.\boldsymbol{x_i}, \tag{4}$$

$$\sum_k{}^{new} = \frac{1}{N_k}\sum_{i=1}^{N} w_{ik}.(\boldsymbol{x_i} - \boldsymbol{\mu_k}^{new}).(\boldsymbol{x_i} - \boldsymbol{\mu_k}^{new})^t \tag{5}$$

Here initialization is done using the K-means algorithm and convergence is checked by observing the log-likelihood of the data using:

$$\log(l(\theta)) = \sum_{i=1}^{N} \log(p(\boldsymbol{x_i}|\boldsymbol{\theta})) \tag{6}$$

Based on the above formula, segmentation process consists of the following steps.

1. Based on the variance of the image, the GMM is applied to segment the pixels into 4 classes corresponding to a) bright pixels showing contusions, hematomas, etc. b) gray-level pixels showing normal tissues, c) white-level pixels showing catheter, etc. and d) pixels belong to white-matter regions. Random initiations are used and segmentation is iteratively carried out till convergence is obtained.
2. Combinations of inputs including original image, denoised image (i.e. output of the Total variation method), the result of the linear contrast stretching and the output of the GMS stage are used as initial set of inputs. In case of non-convergence using the above set of inputs, owing to the high level of granular noise, another set of inputs such as the above set except for the original image is used. If still the GMM does not converge after a predefined number of iterations then the results are submitted for post-processing.

C. *Post-processing*

Post-processing consists of the following stages:

1. Intensity Constraint: In this stage, regions with the highest average intensity are chosen as hematoma is diagnosed in such regions.
2. Area Constraints: In this stage we perform the followings:
   A) Total Area Constraint: Here, it is checked that the total area of the highest average intensity region is not more than a predefined threshold. This condition is checked to reject abnormally bad segmentation results.
   B) Micro Area Constraint: Here, we iteratively reduce the distinct components identified in the region of interest after application of Total Area Constraint. We first identify the smallest disjoint component in the area of interest and remove the areas less than twice its area. Then, we repeat this process iteratively till a maximum of n_a components are left.
3. Midline Pattern Matching: In this stage, the midline that has high intensity value is removed by using a simple rectangular template. This is done to exclude the midline from being detected as Hematoma. This template is constructed by calculating the mass center for the cranial area and defining an appropriate rectangle around it.
4. Bright objects removal: In this stage, objects with the average intensity higher than a predefined threshold are removed using an intensity-cum-size based test on the final distinct regions of hematoma.
5. Edge Removal: The part of the brain being analyzed is derived after extracting the skull region around it. In this process the edge of the skull is retained which might appear as part of hematoma being of higher intensity. The following algorithm is used to remove the outlier edges.
   - The image gradient directions are calculated for all the boundary points of detected hematoma regions.
   - For each point like 'A', the gradient direction is quantized into 8 angular regions. In each direction, the image point at a distance of t_h units from 'A' is checked.
   - If the point also belongs to the hematoma region, then 'A' is left unchanged. If it doesn't belong to the Hematoma region then the point 'A' along with the t_h points in between are dismembered from the desired region.

III. Experimental Results

We used axial CT images with 4.5 to 5mm slice thickness from 11 patients suffered from traumatic brain injury. The images were provided by Virginia Commonwealth Health System. The total number of patients and images are respectively 70 and 3133 and the resolution of each image is 512×512. Among these patients we found 11 cases with hematoma.

Assuming the image is normalized, we assigned 0.1 and 0.9 respectively to t_1 and t_2. Also, both n_a and t_h are set to 5. Figure 2 shows the segmentation results for two images from different patients. As it can be observed from Figure 2, the proposed method is able to detect the hematoma and removes the artifacts and skull from the images. Even though there are other regions in the images with similar pixel values to the hematoma regions, the proposed method identifies those regions and doesn't detect them as hematoma. As instance, in Figure 2.b the midline and the small object close to the center have similar pixel values to hematoma regions. However, these parts are not detected as hematoma in Figure 2.d.

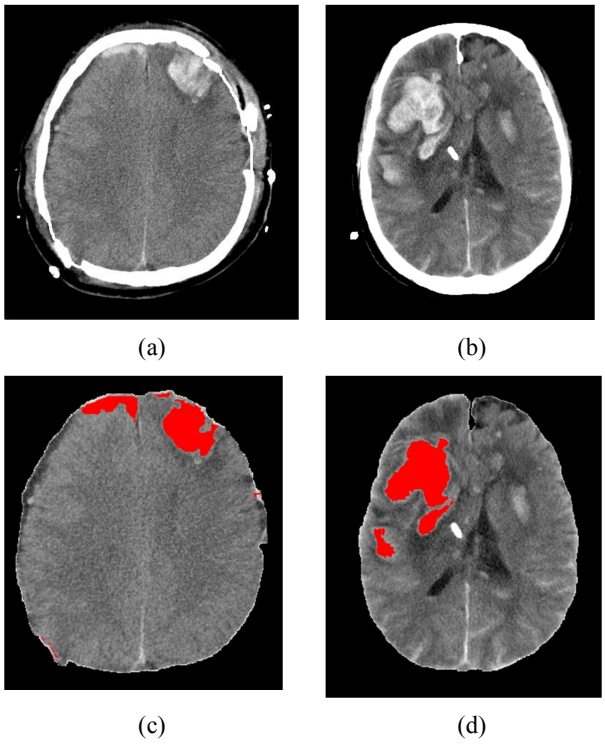

Figure 2. Input images and detected hematoma. (a) and (b) are input images. Red regions show the hematoma in (c) and (d) respectively correspond to (a) and (b).

In order to evaluate the accuracy of the proposed segmentation method we use sensitivity and specificity defined as:

$$Sensitivity = \frac{|A \cap \hat{A}|}{|A \cap \hat{A}| + |A - \hat{A}|} \quad (7)$$

$$Specificity = \frac{|R - (A \cup \hat{A})|}{|R - (A \cup \hat{A})| + |\hat{A} - A|}$$

where $\hat{A}$ and A show the segmented area respectively by the proposed method and the gold standard (i.e. manual segmentation). Also, R shows a set of pixels that belong to brain without skull and without background of the slice. The values of specificity and sensitivity are respectively 0.982, and 0.729.

IV. Conclusion

Traumatic brain injury is a major public health problem with a high percentage of fatality rate and tremendous lifetime costs including medical costs and lost productivity. Severity of the TBI depends on some parameters such as hematoma. In this paper we proposed a method to segment hematoma in CT images of patients suffering from TBI. We first performed pre-processing methods such as "total variation" method for denoising and contrast adjusting to focus on the regions of interest. After that by developing a GMM we segmented the image. As the output of the GMM contained non-relevant regions to the hematoma we performed post-processing to remove those parts. The simulation results showed the accuracy of the proposed method.

Acknowledgment

The authors would like to thank Dr. Charles H. Cockrell for clinical advice on this project. In addition, H. Derksen was supported by NSF grant DMS 1302032.

References

[1] Cozza, Stephen J., Matthew N. Goldenberg, and Robert J. Ursano, eds. Care of Military Service Members, Veterans, and Their Families. American Psychiatric Pub, 2014

[2] P. Vos, and R. Diaz-Arrastia, eds., "Traumatic brain injury," John Wiley & Sons, Ltd, 2014.

[3] W. He, L. S. Wang, H. Z. Li, L. G. Cheng, M. Zhang, and C. G. Wladyka, "Intraoperative contrast-enhanced ultrasound in traumatic brain surgery," *Clinical imaging*, vol. 37, no. 6, pp. 983-988, 2013.

[4] R. Härtl, L.M. Gerber, Q. Ni, and J. Ghajar, "Effect of early nutrition on deaths due to severe traumatic brain injury," *Journal of Neurosurgery*, vol. 109, no.1, pp. 50-56, 2008.

[5] W. Chen, R. Smith, S.Y. Ji, K. Ward, and K. Najarian, "Automated ventricular systems segmentation in brain CT images by combining low-level segmentation and high-level template matching," *BMC medical informatics and decision making,* vol. 9, no. Suppl 1:S4, 2009.

[6] V. Agarwal, and S. A. Tisherman, "Traumatic brain injury," In I*maging the ICU Patient*, pp. 365-375. Springer London, 2014.

[7] E. Kurča, E., Š. Sivák, and P. Kučera, "Impaired cognitive functions in mild traumatic brain injury patients with normal and pathologic magnetic resonance imaging," *Neuroradiology* , vol.48, no. 9, pp. 661-669, 2006.

[8] L. Babcock, T. Byczkowski, S. Mookerjee, and J. J. Bazarian, "Ability of S100B to predict severity and cranial CT results in children with TBI," *Brain injury*, vol. 26, no. 11, pp. 1372-1380, 2012.

[9] L. S. Prichep, R. Naunheim, J. Bazarian, W. A. Mould, and D. Hanley, "Identification of hematomas in mild traumatic brain injury using an index of quantitative brain electrical activity," *Journal of neurotrauma*, vol. 32, no. 1, pp. 17-22, 2015.

[10] M. Soltaninejad, T. Lambrou, A. Qureshi, N. Allinson, and X. Ye., "A hybrid method for haemorrhage segmentation in trauma brain CT," in *Medical Image Understanding and Analysis Conference*, 2014.

[11] B. Prakash, S. Zhou, T. C. Morgan, D. F. Hanley, and W. L. Nowinski, "Segmentation and quantification of intra-ventricular/cerebral hemorrhage in CT scans by modified distance regularized level set evolution technique," *International journal of computer assisted radiology and surgery*, vol. 7, no. 5, pp. 785-798, 2012.

[12] C. Li, C. Xu, Changfeng Gui, and M. D. Fox, "Distance regularized level set evolution and its application to image segmentation," *IEEE Transactions on Image Processing*, vol. 19, no. 12, pp. 3243-3254. 2010.

[13] Y. H. Li, L. Zhang, Q. M. Hu, H. W. Li, F. C. Jia, and J. H. Wu, "Automatic subarachnoid space segmentation and hemorrhage detection in clinical head CT scans," *International journal of computer assisted radiology and surgery,* vol. 7, no. 4, pp. 507-516, 2012.

[14] H. S. Bhadauria, and M. L. Dewal, "Efficient denoising technique for CT images to enhance brain hemorrhage segmentation," *Journal of digital imaging*, vol. 25, no. 6, pp. 782-791, 2012.

[15] Y. Zhang, M. Chen, Q. Hu, and W. Huang, "Detection and quantification of intracerebral and intraventricular hemorrhage from computed tomography images with adaptive thresholding and case-based reasoning," *International journal of computer assisted radiology and surgery*, vol. 8, no. 6, pp. 917-927, 2013.

[16] X. Qi, S. Shandilya, A. Belle, R. Hargraves, C. Cockrell, Y. Tang, K. Ward, and K. Najarian, "Automated analysis of CT slices for detection of ideal midline from brain CT scans." In *International Multi-Conference on Computing in the Global Information Technology*, pp. 117-121, 2013.

[17] L.I. Rudin, S. Osher, and E. Fatemi. "Nonlinear total variation based noise removal algorithms." *Physica D: Nonlinear Phenomena*, vol. 60, no.1-4, pp. 259-268, 1992.

[18] M. Zhu, and T. Chan., "An efficient primal-dual hybrid gradient algorithm for total variation image restoration," UCLA CAM Report 08-34, 2008.

[19] J. L. Gauvain, and C.H. Lee., "Maximum a posteriori estimation for multivariate Gaussian mixture observations of Markov chains," *IEEE Transactions on Speech and audio processing*, vol.2, no.2, pp. 291-298, 1994.